TABLE OF CONTENTS

Volume I

Volume II

Chapter 1

CYCLONE DUST COLLECTORS

I. INTRODUCTION

Cyclone dust collectors are one of the most simple dust collectors, do not have movable parts, and are easy to maintain.

A representative illustration of the flow pattern of air, and of the solid particle separation process in the tangential inlet cyclone, is shown in Figure 1.

The centrifugal force

$$Z \left(= \rho_p \cdot \frac{\pi \cdot Xp^3}{6} \cdot \frac{U\theta^2}{r} \right)$$

acting on a solid particle of diameter Xp rotating with velocity Uθ in a circle of a radius r comes to the centrifugal effect (Z/G) = 300 to 2000 in comparison with the gravity force

$$G = \rho_p \cdot \frac{\pi \cdot Xp^3}{6} \cdot g$$

of the solid particle. In spite of the simple construction of cyclones, solid particles have high centrifugal effect value (= Z/G). The mass of the fine solid particle in the centrifugal field apparently is then equivalent to the heavy particle by the centrifugal effect. Therefore, the cyclone dust collectors are useful for separating fine solid particles in the turbulent rotational air flow.

II. TYPES OF CYCLONES

A. Returned Flow Type of Tangential Inlet Cyclone

Figure 2 shows the conical type of a cyclone which was devised by Morse in 1886. This type of cyclone was mainly applied in the separation of the coarse particles or grains.[1]

Figure 3 shows a Linden type of cyclone which was designed by ter Linden in 1935.[2] In order to introduce the dust-laden gas from the periphery into the cyclone by the homogeneous distribution of the dust-laden gas, the inlet pipe is wound over the cyclone body of diameter D1.

ter Linden recommended that the total length L + H be longer than or equal to 3·D1, and D1 is equal to 2.5·D2.

Figure 4 shows the double entry cyclone which divides the inlet dust-laden gas flow into two parts,[3] one of which flows along the outer wall surface and another of which flows in the annular space between the inner pipe and the middle curved plate.

Figure 5 shows a Liot-cyclone which was designed by an institute of the Soviet Union.[4]

B. Axial Flow Cyclone

There are several problems concerning the separation of solid particles in return flow types of the tangential inlet cyclones:

1. When the turbulent rotational flow is returned in the space of the cone, as shown in Figures 1 and 3, the separated dust has the possibility of escaping from the inner pipe with the upward rotational gas flow.
2. The separated dust particles in the dust bunker have a possibility of escaping from the bunker by the secondary flow in the boundary layer due to the remaining turbulent rotational flow in the dust bunker.

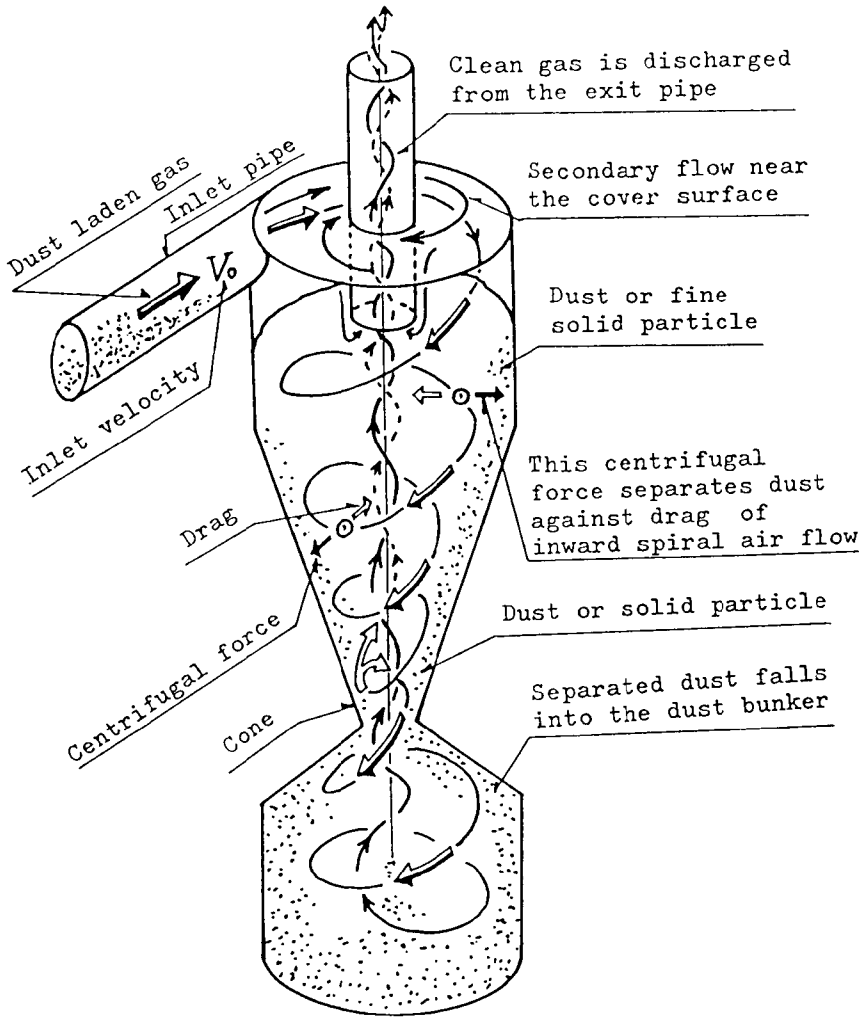

FIGURE 1. Diagram of the flow pattern of the three dimensional spiral flow and of the mechanism of the separation of dust.

In order to correct the above stated defects, the axial flow type of the cyclone was devised. Figure 6 shows the uniflow cyclone which was designed by Umney.[5] The rotational flow is created by the guide vanes. The solid particles are thrown on the outer wall by the centrifugal force in the coaxial space.

The clean gas flows out through the center annular space. This type of cyclone is used in multi-cyclones. The separation efficiency $\eta_c(\%)$ goes down in comparison with the tangential type of the cyclones due to the weak rotational gas flow by means of the guide vanes.

Figure 7 shows a separating unit designed for laminar flow types of cyclones.[6] Radial vanes are set at the center of a cylindrical tube and, assuming that the minimum interval between the inner wall surface of the tube and the outer edges of the radial vanes are d = 12.5 mm or one tenth the diameter of the separating tube of interval diameter of D1 = 125 mm, and also assuming that the gas moves through a separating unit with Vo = 1.5 m/s at a temperature T = 473 K, then the flow Reynolds number Re may be estimated as

$$\mathrm{Re} = \frac{\mathrm{Vo} \cdot d}{\upsilon} \doteqdot 5400$$

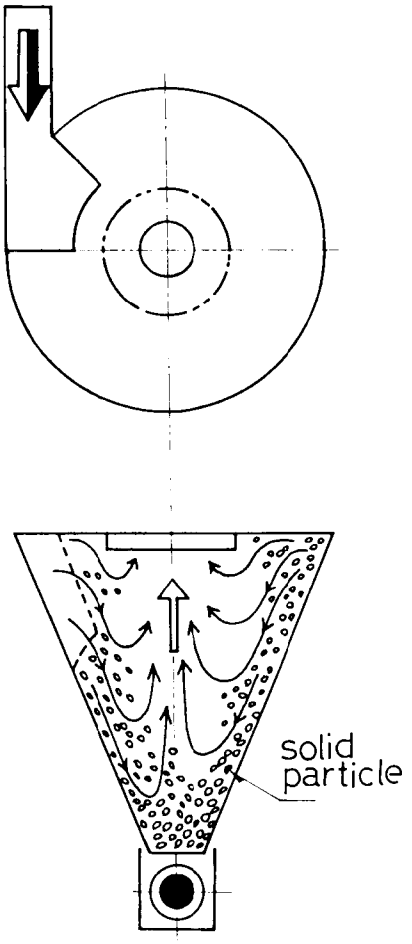

FIGURE 2. Morse-designed cyclone (1886).

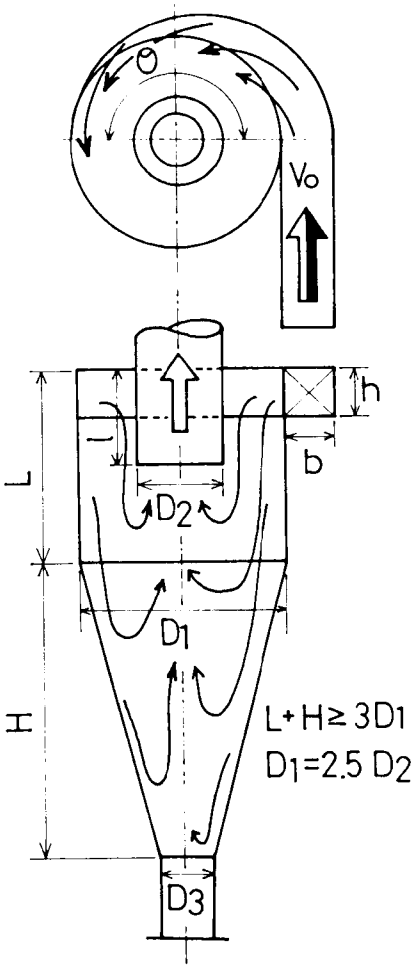

FIGURE 3. Linden cyclone (1935).

Therefore, under these flow conditions, the gas flow may be assumed to be stabilized in a laminar condition as long as the Reynolds number is below approximately 10,000 in centrifugal type separating units[7] (British Patent 713,930). However, according to the hydrodynamical consideration for quasi-free vortex flow in this interval, this type of vortex flow has a tendency to become an unstable flow. Therefore, even if the straight flow may be assumed to be a laminar flow, the spiral flow which is combined with straight flow and vortex flow becomes an unstable flow condition.

A particular advantage of this radial vane form is that the spiral flows are set up by the frictional drag of the main stream rotating in the annular zone around the core in each of the four quadrants of the cross-shaped vanes. The eddy in each quadrant rotates at its outer surface in the same direction as the main flow so that there is little, if any, frictional drag between the main stream and the localized eddy in each quadrant. The effect is to cause the main gas stream to roll around and on the eddy as if rolling on roller bearings.

The result is stability of the main gas flow with a minimum of friction or energy dissipation by virtue of contact with the radial vanes. This fact lends stability to the main gas flow and helps maintain its laminar character. Any dust or solid particles that enter into these rotational flows are thrown out in a short time because the centrifugal force applied to them while in the rotational flow is relatively high.

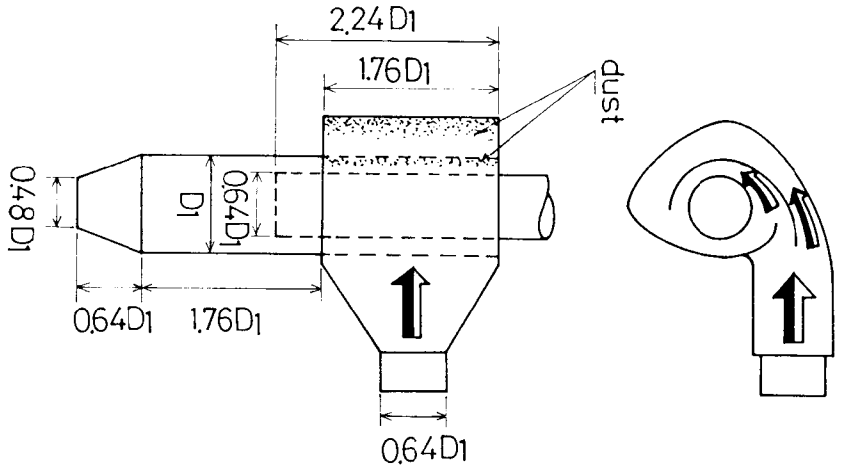

FIGURE 4. Double entry cyclone.

C. Returned Flow Type of Axial Flow Cyclone

Figure 8 shows return flow types of the axial flow cyclones. The dust-laden gas flow axially enters into the cyclone and then begins to rotate after flowing through the guide vanes. The clean gas escapes from the inner pipe. This type of cyclone is applied for multi-cyclones. In Figure 8, the tangential velocity Vo distributions measured by Jotaki[8] in the cyclone are shown, where Vo is the mean inlet velocity.

III. FLOW PATTERN OF GAS

A. Flow Pattern of Gas by Prockat

Figure 9 shows the velocity distributions in the cyclone by Prockat (1930).[9] From these experimental results, it was clear that the velocity distribution of gas in the cyclone was composed of the nearly forced vortex flow in the central region and of the nearly free vortex flow in the outer region.

B. Secondary Flow Pattern

Figure 10 shows the observation of the secondary flow pattern by Hughes (1957).[10] It is very important to recognize that the flow of the short circuit near the surface of the inner pipe occurs by the boundary layer effect. This short circuit remarkably drops the collection efficiency of the dusts.

Figure 11 shows the very interesting double vortex flow in the van Tongeren type of cyclone. This flow pattern was observed by Jackson (1962).[11]

Figure 12 shows the secondary flow pattern in the annular space near the inlet pipe region. Those stream lines were calculated by Liu, Jia, Zhang, Hao, Wang, and Xu (1978).[12]

Figure 13 shows the secondary flow patterns near the inlet pipe region around the space between the outer pipe D1 = 150 mm and the inner pipe D2 = 51 mm in a cylindrical cyclone.[13] The mean inlet velocity Vo in the inlet pipe is Vo = 20 m/s. From this figure, it can be seen that the flow pattern of the secondary flow in the cyclone dust collector is not always the same flow pattern, but changes the flow pattern from the inlet angle θ = 0.89 rad to the transverse angle θ = 3.14 rad. This flow pattern is very important in considering the collection efficiency of fine solid particles.

C. Tangential Velocity Distribution

1. Rankine Combined Vortex

One of the simplest vortex models is Rankine's combined vortex flow which is composed of the forced vortex and the free vortex. The forced vortex can be represented by

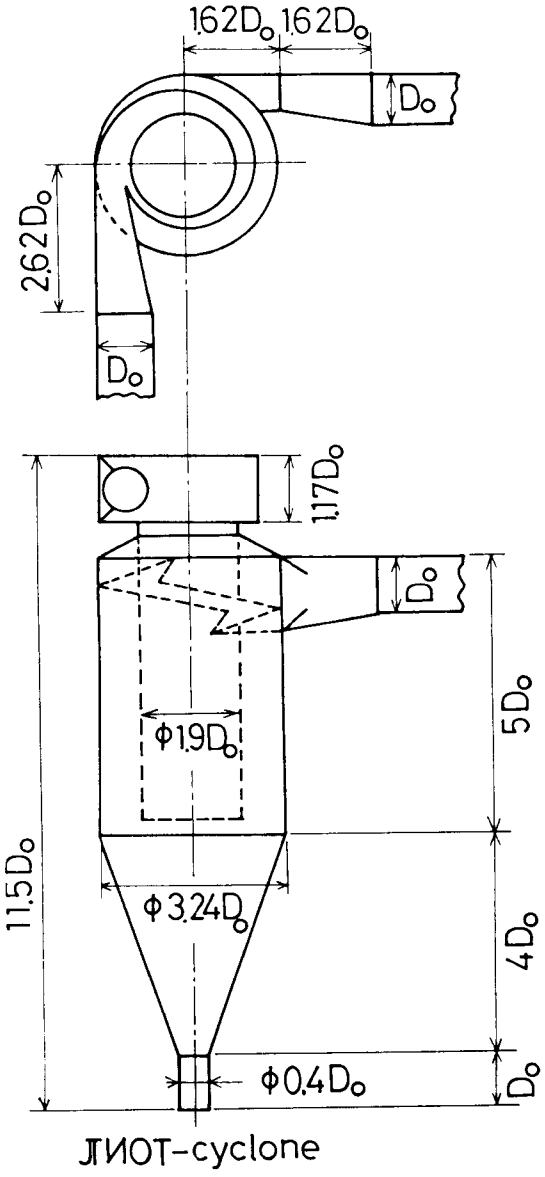

FIGURE 5. Liot-cyclone.

$$V\theta = \omega \cdot r \ (0 \leqq r \leqq a) \tag{1}$$

and the free vortex can be written

$$V\theta \cdot r = \Gamma \ (r \geqq a) \tag{2}$$

where a symbol ω(rad/s) is an angular velocity and a symbol $\Gamma(m^2/s)$ means a circulation. This vortex model is shown in Figure 14. The static pressure distributions can be represented as:

$$p = p_a + \frac{\rho \cdot \Gamma^2}{2} \cdot \left(\frac{1}{a^2} - \frac{1}{r^2} \right) \tag{3}$$

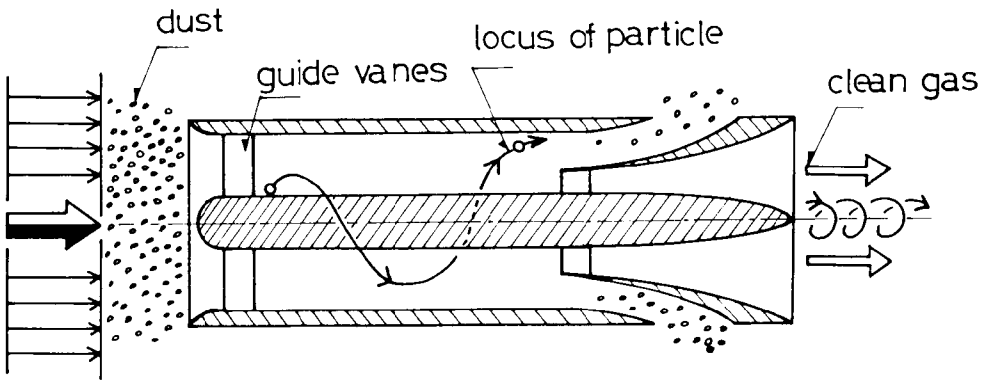

FIGURE 6. Umney cyclone (1948).

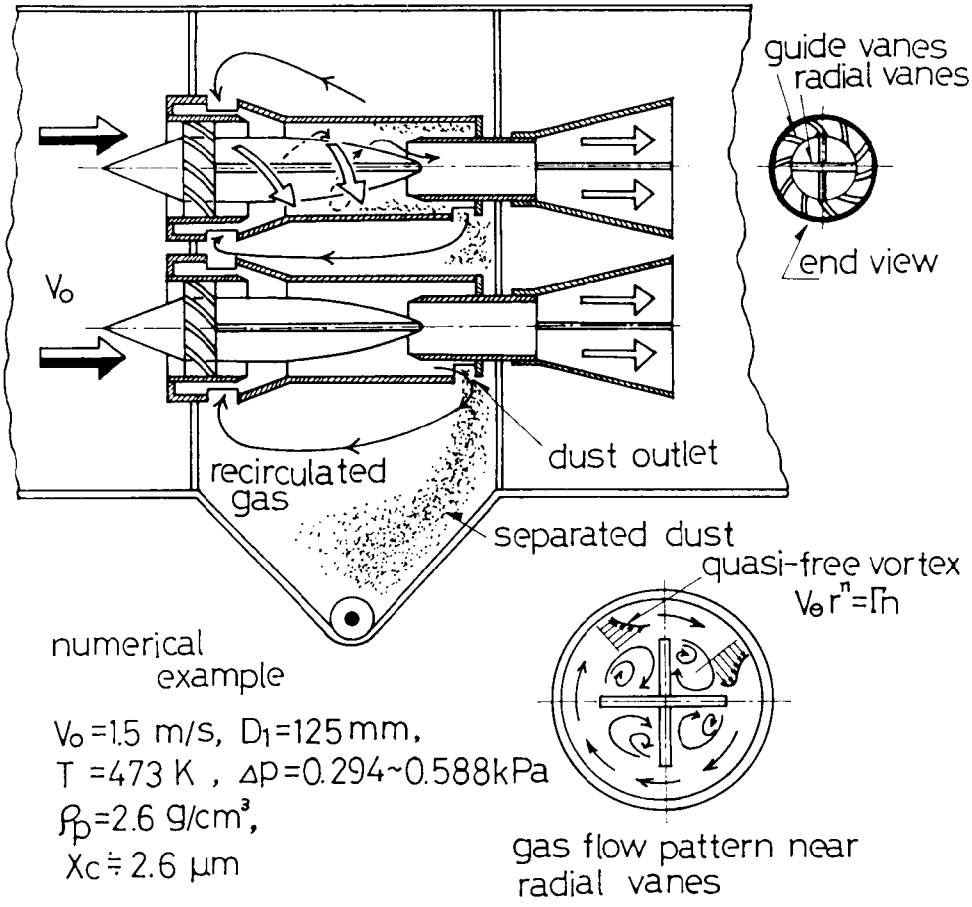

FIGURE 7. Laminar flow cyclone.

and for the free vortex

$$p = p_0 + \frac{\rho \cdot \Gamma^2}{2 \cdot a^4} \cdot r^2 \tag{4}$$

Therefore, the difference of the static pressures $(0 - p_a)$ and $(P_a - P_o)$ is equal to

$$0 - p_a = p_a - p_0 = \frac{\rho \cdot \Gamma^2}{2 \cdot a^2} \tag{5}$$

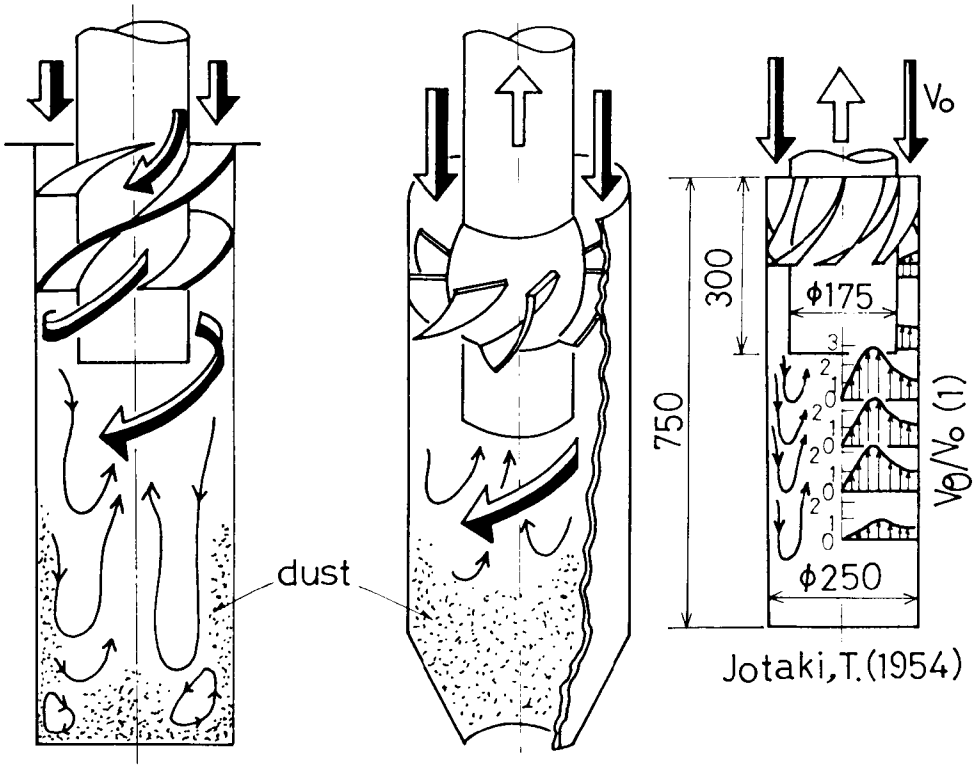

FIGURE 8. Return flow types of the axial flow cyclones.

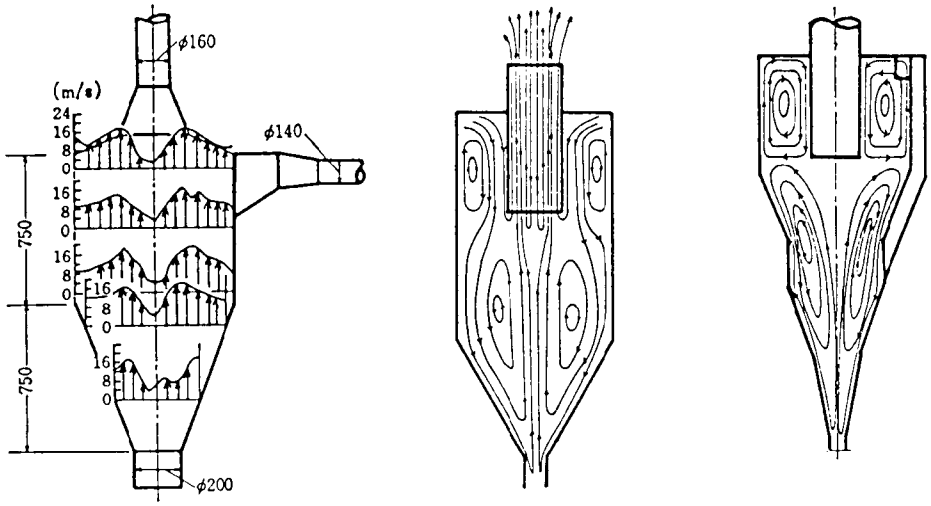

FIGURE 9 (left). Velocity distributions in the cyclone by Prockat (1930). FIGURE 10 (center). Secondary flow in the cyclone by Hughes (1957). FIGURE 11 (right). Double vortex flow in the cyclone by Jackson (1962).

where 0 means atmospheric pressure.

2. Burgers' Vortex Model

In the turbulent rotational flow, namely, a Reynolds stress larger than a viscous stress, Burgers (1948)[14] derived his vortex model by using the Navier-Stokes equation and the

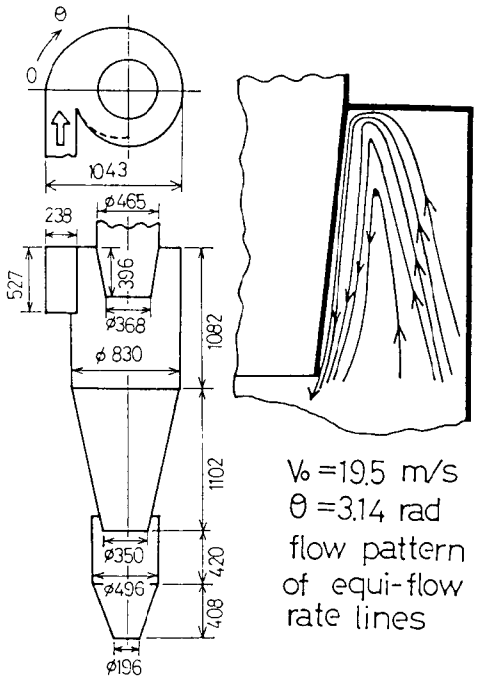

FIGURE 12. Secondary flow pattern (Data from *Acta Mech. Sin.*, 3, 182, 1978.).

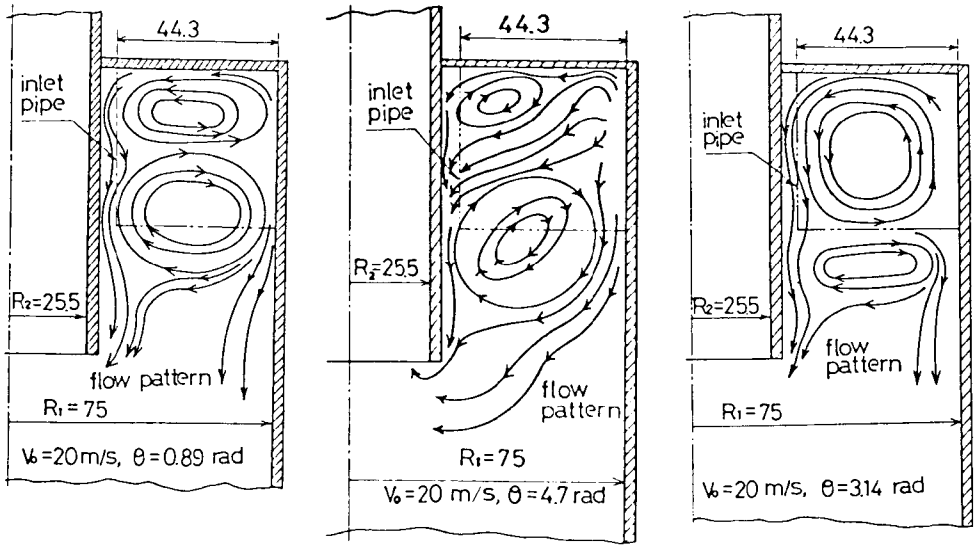

FIGURE 13. Secondary flows near the inlet pipe region.

continuity equation. Denoting that the tangential and radial velocities at the radius r = b are Vθb and Vrb, respectively, then the dimensionless radius r′ = r/b, the dimensionless velocities Vθ′ = Vθ/Vθb, and then Vr′ = Vr/Vrb are introduced, so the equations of the tangential and radial velocities in the radius region $0 \leqq r \leqq b$ can be represented as

$$V'_\theta = \frac{1}{r'} \frac{1 - \exp(-\mathrm{Reb} \cdot r'^2/2)}{1 - \exp(-\mathrm{Reb}/2)} \tag{6}$$

$$V'_r = r' \tag{7}$$

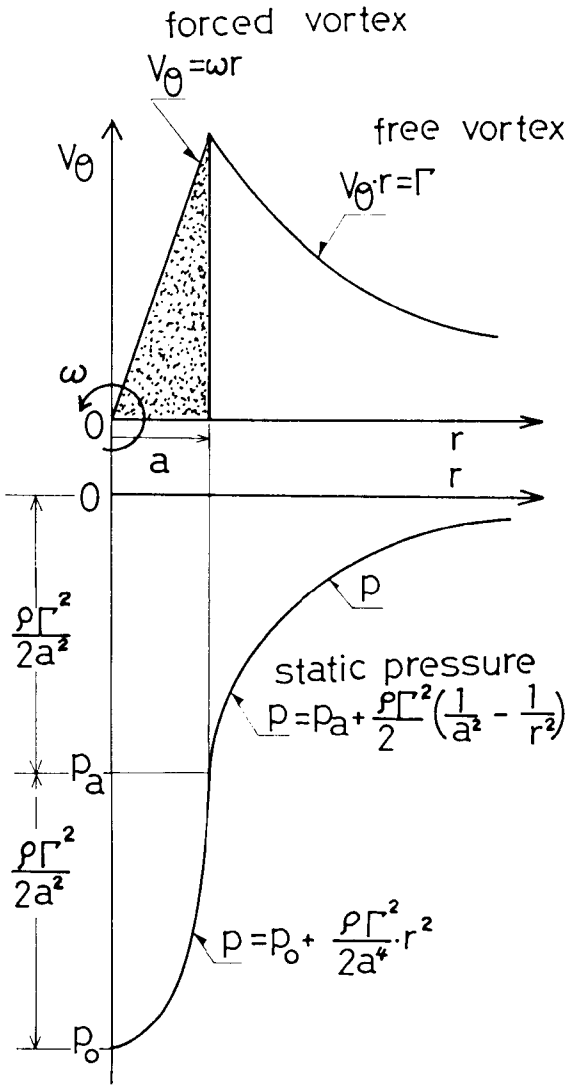

FIGURE 14. Rankine combined vortex model.

where the dimensionless symbol Reb means a Reynolds number defined as

$$\text{Reb} = \frac{-b \cdot Vrb}{\upsilon_T} \tag{8}$$

The symbol $\upsilon_T(m^2/s)$ means an eddy kinematic viscosity.

Distribution curves of Equation 6 of Burgers' vortex model are shown in Figure 15 for the various kinds of the Reynolds number Reb. In the figures, the symbols ○,△,□,●,▲ are the measured tangential velocities in the cyclone of D1 = 150 mm, D2 = 50 mm, and Do = 50 mm. Figure 16 shows the velocity distribution of Burgers' vortex model for Reb = 20. The measured velocities are shown for D1 = 150 mm, D2 = 50 mm, and Do = 50 mm. In addition, the velocity distribution near the outer wall surface measured by Muschelknautz and Krambrock (1970) is shown.

Figure 17 shows the distributions of the eddy kinematic viscosity for the inlet velocity of

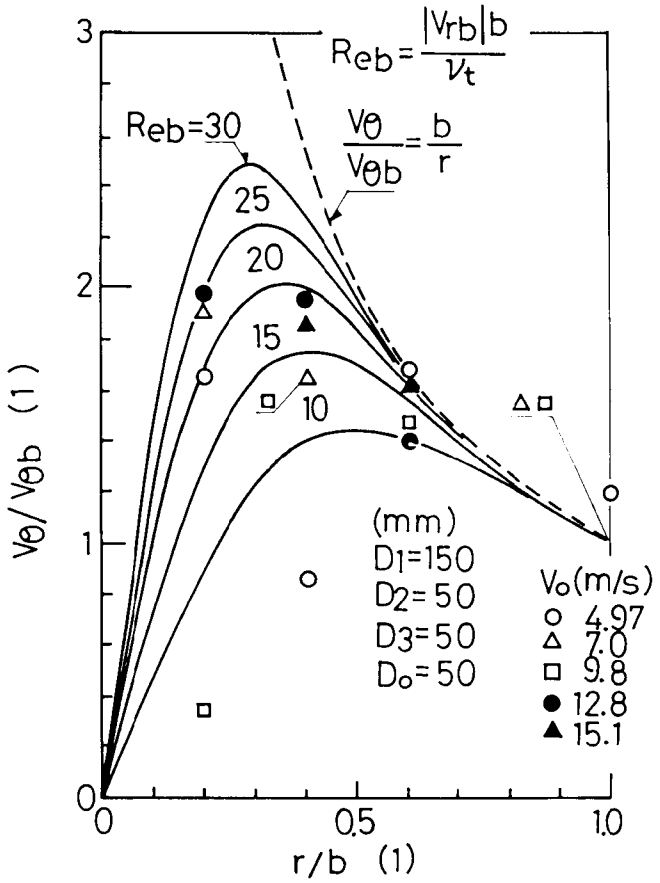

FIGURE 15. Burgers' vortex flow distributions.

air Vo = 5, 7, 10, 13, and 15 m/s in the vortex chamber of D1 = 141 mm and $H_T \fallingdotseq 380$ mm. Those values of υ_T/υ were measured with the hot-wire of X-probe by Ogawa and Fujita (1981). The maximum value of υ_T/υ is located in the quasi-forced vortex region.

Figure 18 shows Prandtl mixing length l in the vortex chamber of Figure 17. In order to estimate the mixing length l, the following equation was applied by Ogawa and Fujita defined as

$$\tau_T = -\rho\cdot\overline{v_r\cdot v_\theta} = \rho\cdot l^2\cdot\left(\frac{dV\theta}{dr} - \frac{V\theta}{r}\right)^2 \qquad (9)$$

From the results of the mixing length of Figure 18, Ogawa (1981) derived the equation of the mixing length l in the confined vortex chamber as

$$\frac{l}{R1} = 6\times 10^{-6}\cdot Rcy\cdot\frac{r}{R1} \qquad (10)$$

where a symbol Rcy is the cyclone Reynolds number defined as

$$Rcy = \frac{Qo}{Hi\cdot\upsilon} \qquad (11)$$

Qo(m^3/s) is the flow rate of gas into the vortex chamber and Hi(m) is the effective length of the imaginary cylinder in the vortex chamber or cyclone.

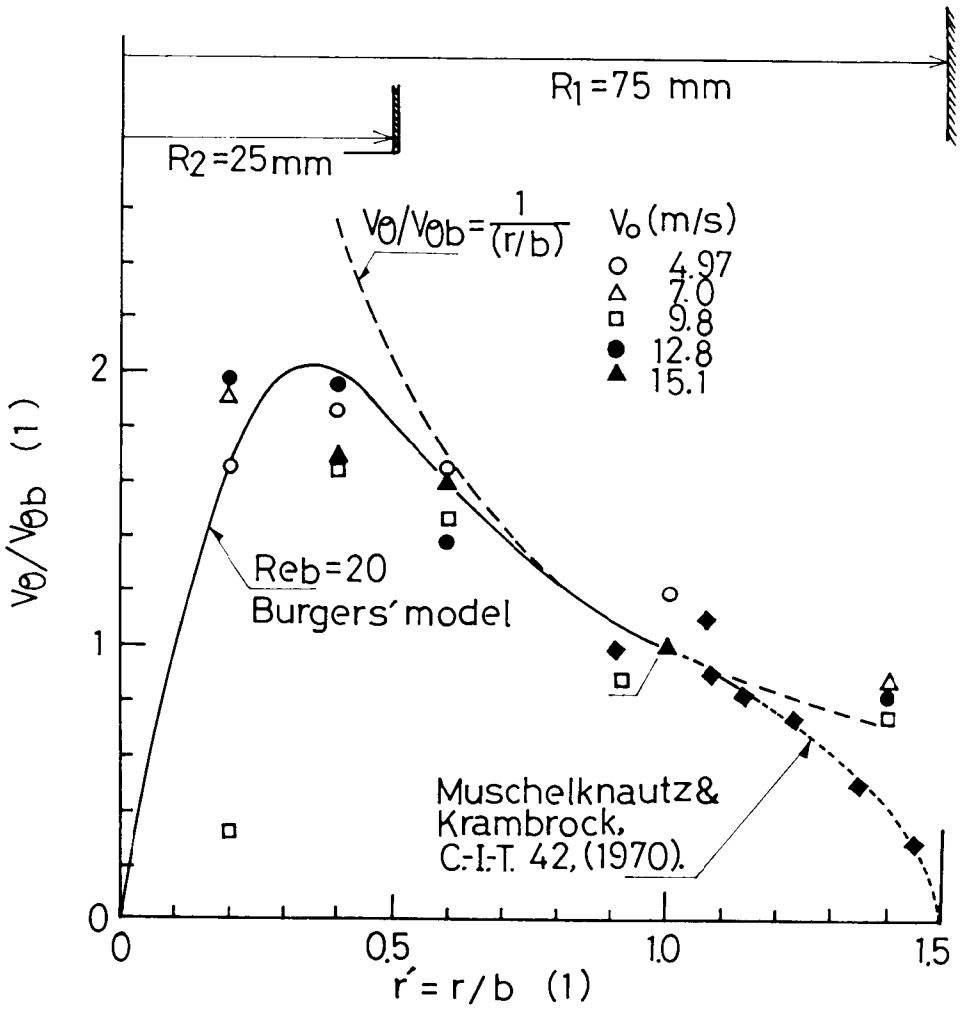

FIGURE 16. Tangential velocity distributions by Burgers vortex flow and Muschelknautz and Krambrock.

3. Ogawa's Combined Vortex

Ogawa's combined vortex model is composed of the quasi-forced vortex ($0 \leqq r \leqq r_t$) and quasi-free vortex ($r \geqq r_t$) defined as

$$V\theta = K \cdot r \cdot \exp(-\Lambda r) \fallingdotseq K \cdot r(1 - \Lambda \cdot r), \quad Vr = -f \cdot r \tag{12}$$

for the quasi-forced vortex

$$V\theta \cdot r^n = \Gamma n, \quad Vr = -\frac{m}{r} \tag{13}$$

where the symbols f(1/s) and m(m^2/s) are constant values and the relationship between Λ, r_t, a, and n are written

$$\Lambda \cdot r_t = \frac{1+n}{2+n}, \quad a \cdot \Lambda = \frac{1}{2} \tag{14}$$

Then a symbol r_t (m) means the boundary radius between the quasi-forced and quasi-free vortices, and n(1) means the velocity index. The value of n is equal to 1 for the potential